

**Persistent expression of the full genome of hepatitis C virus in B cells induces
spontaneous development of B-cell lymphomas *in vivo***

Yuri Kasama^{1,6}, Satoshi Sekiguchi^{2,6}, Makoto Saito¹, Kohsuke Tanaka¹, Masaaki Satoh¹,
Kazuhiko Kuwahara³, Nobuo Sakaguchi³, Motohiro Takeya⁴, Yoichi Hiasa⁵, Michinori
Kohara², and Kyoko Tsukiyama-Kohara¹

¹Department of Experimental Phylaxiology, Faculty of Life Sciences, Kumamoto University,
Kumamoto 860-8556, Japan.

²Department of Microbiology and Cell Biology, Tokyo Metropolitan Institute of Medical
Science, Tokyo 113-8613, Japan.

³Department of Immunology, Faculty of Life Sciences, Kumamoto University, Kumamoto
860-8556, Japan.

⁴Department of Cell Pathology, Faculty of Life Sciences, Kumamoto University, Kumamoto
860-8556, Japan.

⁵Department of Gastroenterology and Metabology, Ehime University Graduate School of Medicine, To-on, Ehime 791-0295, Japan.

⁶These authors contributed equally to this work.

Short title: HCV expression in B cells induces B-cell lymphoma

Abstract word count: 199

Text word count: 2,828

ABSTRACT

Extrahepatic manifestations of hepatitis C virus (HCV) infection have been reported in 40–70% of HCV-infected patients. B-cell non-Hodgkin’s lymphoma is a typical extrahepatic manifestation frequently associated with HCV infection. Although the HCV infection of B cells has been reported, the mechanism of disease onset remains unclear. In this study we established HCV transgenic mice that express the full HCV genome in B cells (RzCD19Cre mice) and observed a 25.0% incidence of non-Hodgkin’s diffuse large B-cell lymphomas (22.2% in males and 25.9% in females) within 600 days after birth. Expression levels of aspartate aminotransferase, alanine aminotransferase, and 32 different cytokines, chemokines and growth factors were examined. The incidence of B-cell lymphoma was significantly correlated with only the level of soluble interleukin-2 receptor α subunit (sIL-2R α) in RzCD19Cre mouse serum. All RzCD19Cre mice with substantially elevated serum sIL-2R α levels (>1,000 pg/mL) developed B-cell lymphomas. Moreover, compared to tissues from control animals, the B-cell lymphoma tissues of RzCD19Cre mice expressed significantly higher levels of IL-2R α . We show that the expression of HCV in B cells promotes non-Hodgkin’s-type

diffuse B-cell lymphoma, and therefore, the RzCD19Cre mouse is a powerful model to study the mechanisms related to the development of HCV-associated B-cell lymphoma.

Introduction

Over 175 million people worldwide are infected with hepatitis C virus (HCV), a positive-strand RNA virus that infects both hepatocytes and peripheral blood mononuclear cells.¹ Chronic HCV infection may lead to hepatitis, liver cirrhosis, hepatocellular carcinomas,^{2,3} and lymphoproliferative diseases such as B-cell non-Hodgkin's lymphoma and mixed-cryoglobulinemia.^{1,4-6} B-cell non-Hodgkin's lymphoma is a typical extrahepatic manifestation frequently associated with HCV infection.⁷ Although infection of B cells by HCV has been reported,⁸ the mechanism of disease onset remains unclear. We previously developed a transgenic mouse model that conditionally expressed HCV cDNA, including the viral genes that encode the core, E1, E2 and NS2 proteins, using the Cre/loxP system (in CN2 mice).^{9,10} The conditional transgene activation of the HCV cDNA (core, E1, E2 and NS2) protected mice from Fas-mediated lethal acute liver failure by inhibiting cytochrome c release from mitochondria.¹⁰ In HCV-infected mice, persistent HCV protein expression is established

by targeted disruption of *irf-1*, and high incidences of lymphoproliferative disorders have been observed in CN2 *irf-1*^{-/-} mice.¹¹ Infection and replication of HCV also occur in B cells,^{12,13} however, the direct effects, particularly *in vivo*, of HCV infection on B cells have not been clarified.

To define the direct effect of HCV infection on B cells *in vivo*, we crossed transgenic mice with an integrated full-length HCV genome (Rz) under the conditional *Cre/loxP* expression system with mice expressing the Cre enzyme under transcriptional control of the B lineage-restricted gene *CD19*,¹⁴ we addressed the effects of HCV transgene expression in this study.

Methods

Animal experiments

Wild-type (WT), Rz, CD19Cre and RzCD19Cre mice (129/sv, BALB/c and C57BL/6J mixed background) were maintained in conventional animal housing under specific pathogen-free conditions. All animal experiments were performed according to the guidelines

of the Tokyo Metropolitan Institute of Medical Science or the Kumamoto University Subcommittee for Laboratory Animal Care. The protocol was approved by the Institutional Review Boards of both facilities.

Measurements of HCV protein and RNA

Mice were anesthetized and bled, and tissues (spleen, lymph nodes, liver and tumors) were homogenized in lysis buffer (1% SDS; 0.5% (w/v) NP40; 0.15 M NaCl; 10 mM Tris, pH 7.4) using a Dounce homogenizer. The concentration of HCV core protein in tissue lysates was measured using an HCV antigen ELISA (Ortho).¹⁵ HCV mRNA was isolated by a guanidine thiocyanate protocol using ISOGEN (Nippon gene) and was detected by RT-PCR amplification using primers specific for the 5' UTR of the *HCR6* sequence.^{16,17} Reverse transcription was performed using Superscript III reverse transcriptase (Invitrogen) with random primers. PCR primers NCR-F 5'-TTCACGCAGAAAGCGTCTAGCCAT-3' and NCR-R 5'-TCGTCCTGGCAATTCCGGTGTACT-3' were used for the first round of HCV cDNA amplification, and the resulting product was used as a template for a second round of

amplification using primers NCRF INNER 5'-TTCCGCAGACCACTATGGCT-3' and NCR-R INNER 5'-TTCCGCAGACCACTATGGCT-3'.

Collection of serum for chemokine ELISA

Blood samples were collected from the supraorbital veins or by heart puncture of sacrificed mice. Blood samples were centrifuged at $10,000 \times g$ for 15 min at 4°C to isolate the serum.¹⁸ Serum concentrations of IL-1 α , IL-1 β , IL-2, IL-3, IL-4, IL-5, IL-6, IL-9, IL-10, IL-12p40, IL-12p70, IL-13, IL-17, Eotaxin, G-CSF, GM-CSF, IFN- γ , KC, MCP-1, MIP-1 α , MIP-1 β , RANTES, TNF- α , IL-15, FGF-basic, LIF, M-CSF, MIG, MIP-2, PDGF β and VEGF were measured using the Bio-Plex Pro assay (Bio-Rad). Serum sIL-2R α concentrations were determined by ELISA (DuoSet ELISA Development System, R&D Systems). Serum aspartate aminotransferase (AST), alanine aminotransferase (ALT) activities were determined using a commercially available kit (Transaminase CII test; Wako).

Histology and immunohistochemical staining

Mouse tissues were fixed with 4% formaldehyde (Mildform 10 N, Wako Pure Chemical Industries), dehydrated with ethanol, embedded in paraffin, sectioned (10 μm thick) and stained with hematoxylin-eosin. For tissue immunostaining, paraffin was removed from the sections using xylene and following the standard method, and sections were incubated with anti-CD3 or anti-CD45R (Santa Cruz Biotechnology) in PBS without Ca^{2+} and Mg^{2+} (pH 7.4) but with 5% skim milk. Next, the sections were incubated with biotinylated anti-rat IgG (1:500), followed by incubation with horseradish peroxidase-conjugated avidin-biotin complex (HRP-ABC; Dako Corp.), and the color reaction was developed using 3,3'-diaminobenzidine. Sections were observed under an optical microscope (Carl Zeiss).

Detection of Ig gene rearrangements by PCR

Genomic DNA was isolated from tumor tissues, and PCR was performed as described¹⁹. In brief, PCR reaction conditions were: 98°C for 3 minutes; 30 cycles at 98°C for 30 seconds, 60°C for 30 seconds, and 72°C for 1.5 minutes; and 72°C for 10 minutes. Mouse V κ genes were amplified using previously described primers.²⁰ Amplification of mouse V λ genes was

performed using Vκcon (5'-GGCTGCAGSTTCAGTGGCAGTGGRTCWGRAC-3'; R, purine; W, A or T) and Jκ5 (5'-TGCCACGTCAACTGATAATGAGCCCTCTC-3'), as described.²¹

Results

Establishment of transgenic mice with the B lineage-restricted HCV gene expression

We defined the direct effect of HCV infection on B cells *in vivo* by crossing transgenic mice that had an integrated full-length HCV genome (Rz) under the conditional *Cre/loxP* expression system (Figure 1A, upper schematic)^{9,16,22} with mice that expressed the Cre enzyme under transcriptional control of the B lineage-restricted gene *CD19*¹⁴ (RzCD19Cre; Figure 1a, lower schematic). Expression of the HCV transgene in RzCD19Cre mice was confirmed by ELISA (Figure 1B); a substantial level of HCV core protein was detected in the spleen (370.9 ± 10.2 pg/mg total protein), but levels were lower in the liver (0.32 ± 0.03 pg/mg) and plasma (not detectable). Reverse transcription (RT)-PCR analysis of peripheral blood lymphocytes (PBLs) from RzCD19Cre mice indicated the presence of HCV transcripts (Figure 1C). The weights of RzCD19Cre, Rz (with the full HCV genome transgene alone), CD19Cre (with the Cre gene knock-in at the CD19 gene locus), and wild-type (WT) mice were measured weekly for more than 600 days post birth; there were no significant differences between these groups (data not shown; the total number of transgenic and WT mice was approximately 200). The survival rate in each group was also measured for >600

days (Figure 1D); survival in the female RzCD19Cre group was lower than that of the other groups.

The spontaneous development of B-cell lymphomas in the RzCD19Cre mouse

At 600 days post birth, mice (n = 140) were sacrificed by bleeding under anesthesia, and tissues (spleen, lymph node, liver, and tumors) were excised and examined by hematoxylin and eosin staining (Figure 2A, Supplementary Figure 1). The incidence of B-cell lymphoma in RzCD19Cre mice was 25.0% (22.2% in males and 29.6% in females) and was significantly higher than the incidence in the HCV-negative groups (Table 1). The incidences of other spontaneous tumors in the RzCD19Cre mice (females: hepatocellular carcinoma, 7.4%; mammary tumor, 7.4%; sarcoma, 7.4%; hematoma, 3.7%; T-cell lymphoma, 7.4%; males: hepatocellular carcinoma, 11.1%; T-cell lymphoma, 2.2%) were not significantly higher than the incidences in the HCV-negative groups (Incidence of spontaneous tumors in these groups; Rz males: hepatocellular carcinoma, 5.9%; Rz females: T-cell lymphoma, 5.9%; CD19Cre females: hematoma, 8.3%; T-cell lymphoma, 5.9%; WT females: T-cell lymphoma, 14.3%) but were markedly lower than the incidence of B-cell lymphoma in RzCD19Cre mice (Table 1; data not shown). The B-cell lymphoma characteristics are shown in Figure 2A and

Supplementary Figure 1; because nodular proliferation of CD45R-positive atypical lymphocytes was observed, lymphomas were diagnosed as typical non-Hodgkin's diffuse B-cell lymphomas (Figure 2A, subpanels d, f, g), Supplementary Figs. 1b, e, h, m). Mitotic cells were also positive for CD45R (Figure 2A, subpanel f, arrowheads). CD3-positive T-lymphocytes were small and had a scattered distribution. Intrahepatic lymphomas had the same immunophenotypic characteristics as B-cell lymphomas (Supplementary Figs. 1k, arrowheads, inset: l-n, RzCD19Cre mouse ID No. 24-4); lymphoma tissues were markedly different compared with the control lymph node (Figure 2A, subpanels a, c, e, ID No. 47-4, CD19Cre mouse) and liver (Supplementary Figure 1j, ID No. 24-2, Rz mouse; tissues were from a littermate of the mice used to generate the data in Supplementary Figure 1d-i, k-n). All samples were reviewed by at least two expert pathologists and classified according to the World Health Organization (WHO) classification.²³ Lymphomas were mostly CD45R positive and identified in the mesenteric lymph nodes (Figure 2A, Supplementary Figure 1), and some were identified as intrahepatic lymphomas (incidence, 4.2%; Supplementary Figure 1k-n). HCV gene expression was detected in all B-cell lymphomas of RzCD19Cre mice (Figure 2B).

To examine the Ig gene configuration in the B-cell lymphomas of the RzCD19Cre mice, genomic DNA was isolated and analyzed by PCR. Ig gene rearrangements were identified in each case (Figure 2C). Genomic DNA isolated from the tumors of a germinal center-associated nuclear protein (GANP) transgenic mouse (GANP Tg#3) yielded a predominant Jk5 PCR product (Figure 2C, V κ -J κ); a predominant JH1 product and a minor JH2 product (Supplementary Figure 2, DH-JH) were also identified, as previously reported¹⁹, indicating that the lymphoma cells proliferated from the transformation of an oligo B-cell clone. The B-cell lymphomas of eight RzCD19Cre mice (mouse ID Nos. 24-1, 54-1, 56-5, 69-5, 42-4, 43-4, 36-3 (data not shown), and 62-2 (data not shown)) yielded a J κ -5 gene amplification product, and the lymphomas from three other mice had the alternative gene configurations J κ -1 (mouse ID No. 31-4), J κ -2 (mouse ID No. 24-4) and J κ -3 (mouse ID No. 42-4; Figure 2C). PCR amplification products from the JH4 (mouse ID Nos. 24-1, 24-4, 54-1, 43-4, 56-5, 69-5, 62-2 (data not shown), 36-3 (data not shown)), JH1 (mouse ID Nos. 31-4, 42-4), and JH3 (mouse ID Nos. 31-4, 42-4, 56-5, 43-4, 36-3 (data not shown)) genes were also detected (Supplementary Figure 2). The mutation frequencies in the J κ -1, -3 and -5 genes were the same as the mutation frequency in the genomic V-region gene¹⁹. Few or no

sequence differences in the variable region were identified among clones from which DNA was amplified. These results indicate the possibility that tumors judged as B-cell lymphomas based on pathology criteria were derived from the transformation of a single germinal center of B-cell origin.

The levels of cytokines and chemokines in the B-cell lymphomas and other tumors of RzCD19Cre mice or tumor-free control mice.

Abnormal induction of cytokine production occurs in HCV-associated non-Hodgkin's lymphomas^{24,25} and in patients with chronic hepatitis.^{26,27} Therefore, we examined tumor cytokine and chemokine levels using a multi-suspension array system (Figure 3). The levels of IL-1 α , IL-1 β , IL-2, IL-3, IL-4, IL-5, IL-6, IL-9, IL-10, IL-12p40, IL-12p70, IL-13, IL-17, Eotaxin, G-CSF, GM-CSF, IFN- γ , KC, MCP-1, MIP-1 α , MIP-1 β , RANTES, TNF- α , IL-15, FGF-basic, LIF, M-CSF, MIG, MIP-2, PDGF β and VEGF were measured in sera from mice with B-cell lymphomas, T-cell lymphomas and other tumors, and in sera from tumor-free RzCD19Cre, Rz, CD19Cre and WT control mice (Figure 3). The levels of IL-12 (p40) and M-CSF in the RzCD19Cre mice with B-cell lymphomas were significantly higher than in the tumor-free controls (IL-12 (p40), $p < 0.0005$; M-CSF, $p < 0.033$). However, the serum IL-12

(p40) and M-CSF levels in other mice (Rz, CD19Cre and WT) with B-cell lymphomas or in RzCD19Cre and Rz mice with other tumors were also significantly higher than in the tumor-free controls ($p < 0.05$). Increased IL-12 (p40) and M-CSF were, therefore, not associated with HCV expression. By contrast, the levels of IL-1 α , IL-1 β , IL-2, IL-12 (p70), IL-17, MIP-1 α and VEGF were significantly lower in the RzCD19Cre mice with B-cell lymphomas than in the tumor-free control mice ($p < 0.05$), and these values were also significantly lower in mice with T-cell lymphomas compared with the values in the tumor-free controls ($p < 0.05$; Figure 3). The levels of other cytokines and chemokines in sera from the tumor-bearing RzCD19Cre mice with B-cell lymphomas were not significantly different compared to those of the control groups, and thus, changes in the expression of these cytokines and chemokines were not strictly correlated with the occurrence of B-cell lymphoma in RzCD19Cre mice.

The levels of amino transferases and soluble IL-2 receptor α in mice lacking or harboring B-cell lymphomas

As described in the methods, we also examined the levels of aspartate amino transferase (AST) and alanine amino transferase (ALT) in the RzCD19Cre, Rz, CD19Cre and WT mice.

There were no significant differences in the levels of AST and ALT in the sera of mice lacking or harboring B-cell lymphomas ($p > 0.05$; Figs. 4a, b; AST: RzCD19Cre mice with B-cell lymphomas, 72.2 ± 60.5 IU/L; normal controls, 55.2 ± 23.0 IU/L; and ALT: RzCD19Cre mice with B-cell lymphomas, 14.2 ± 3.1 IU/L; normal controls, 11.5 ± 3.0 IU/L).

Finally, we examined the level of soluble IL-2 receptor α (sIL-2R α) in the sera of the RzCD19Cre mice with B-cell lymphomas; sIL-2R α is generated by proteolytic cleavage of the IL-2R α (CD25) residing on the surface of activated T and natural killer cells, monocytes, and certain tumor cells.^{21,28} The average sIL-2R α level in the RzCD19Cre mice with B-cell lymphomas (830.3 ± 533.0 pg/mL) was significantly higher than that in the tumor-free control groups, including the RzCD19Cre, Rz, CD19Cre, and WT mice (499.9 ± 110.2 pg/mL; $p < 0.0057$; Figure 4C). The average sIL-2R α levels in other tumor-containing groups (430.46 ± 141.15 pg/mL) were not significantly different from those in the tumor-free control groups ($p > 0.05$; Figure 4C). Moreover, all RzCD19Cre mice with a relatively high level of sIL-2R α ($>1,000$ pg/mL) presented with B-cell lymphomas (Figure 4C).

Expression of IL-2R α in B cell lymphomas of the RzCD19Cre mice

To examine whether sIL-2R α was derived from lymphoma tissues, we quantified IL-2R α concentrations in splenocytes, PBLs and B-cell lymphoma tissues (Figure 5). The concentration of IL-2R α was significantly higher in splenocytes from RzCD19Cre mice compared with those from CD19Cre mice; the concentration was even higher in B-cell lymphoma tissues than in splenocytes from RzCD19Cre mice (Figure 5). These results strongly suggest that B-cell lymphomas directly contribute to the elevated serum concentrations of sIL-2R α in RzCD19Cre mice (Figure 4C, 5).

Discussion

We have established HCV transgenic mice that have a high incidence of spontaneous B-cell lymphomas. In this animal model, the HCV transgene is expressed during the embryonic stage, and these RzCD19Cre mice are expected to be immunotolerant to the HCV transgene product. Thus, the results in this study revealed the potential of the HCV gene to induce B-cell lymphomas without inducing host immune responses against the HCV gene product. A retrospective study indicated that viral elimination reduced the incidence of malignant lymphoma in patients infected with HCV.²⁹ The results in our study may be

consistent with this retrospective observation, indicating the significance of the direct effect of HCV infection on B-cell lymphoma development.

Recent findings have revealed the significance of B lymphocytes in HCV infection of liver-derived hepatoma cells.³⁰ In 4.2% of the RzCD19Cre mouse, CD45R-positive intrahepatic lymphoma was identified, and infiltration of B-cells to the hepatocytes was frequently observed (data not shown). These phenomena might suggest that HCV could modify the *in vivo* tropism of B-cells, and the RzCD19Cre mouse is a powerful model system to address these mechanisms *in vivo*.

As a circulating membrane receptor, sIL-2R α is localized in lymphoid cells and some other types of cancer cells and is highly expressed in several cancers³¹⁻³⁶ and autoimmune diseases.³⁷ Recent findings indicate the link between sIL-2R α levels and hepatocellular carcinoma in Egyptian patients.³⁸ Appearing on the surface of leukemic cells derived from B and pre-B lymphocytes and other leukemic cells, IL-2R α is one of the subunits of the IL-2 receptor, which is composed of an α chain (CD25), a β chain (CD122) and a γ chain (CD132).³⁹ IL-2R ectodomains are thought to be proteolytically cleaved from the cell surface^{30,40,41} and not produced as a result of posttranscriptional splicing.²¹ In RzCD19Cre

splenocytes, the level of IL-2R α was higher than those in the CD19Cre mouse; however, serum concentration of sIL-2R α in the RzCD19Cre mouse without B-cell lymphoma did not show significant differences compared with other control groups (Rz, CD19Cre and WT).

These results indicate the possibility that HCV may increase the IL-2R α expression on B-cells; the proteolytic cleavage of IL-2R α was increased after the B-cell lymphoma development in the RzCD19Cre mouse. The detailed mechanism to induce IL-2R α by HCV is still unclear at present, but we found previously that the HCV core protein induced IL-10 expression in mouse splenocytes.¹¹ IL-10 upregulates the expression of IL-2R α (Tac/CD25) on normal and leukemic B lymphocytes,⁴² and therefore, through IL-10, the HCV core protein might induce the IL-2R α in B cells of the RzCD19Cre mouse.

In conclusion, this study established an animal model that will likely provide critical information for the elucidation of molecular mechanism(s) underlying the spontaneous development of non-Hodgkin's B-cell lymphoma following HCV infection. This knowledge should lead to therapeutic strategies to prevent the onset and/or progression of B-cell lymphomas.

Acknowledgements

We thank Dr. T. Ito for assistance with pathology characterization. This work was supported by grants from the Ministry of Health and Welfare of Japan and the Cooperative Research Project on Clinical and Epidemiological Studies of Emerging and Re-emerging Infectious Diseases.

Authorship Contribution

Contribution: K.T.-K. conceived of the project. Y.K., S.S., M.S., K.T., M.S., M.T. and K.T.-K. performed experiments and analyses. K.K., M.K. and K.T.-K. designed the studies. N.S. and Y.H. provided scientific advice, and K.T.-K. wrote the manuscript.

Conflict-of-interest disclosure: The authors declare no competing financial interests.

Correspondence: Kyoko Tsukiyama-Kohara, Department of Experimental Phylaxiology, Faculty of Life Sciences, Kumamoto University, Kumamoto 860-8556, Japan.

kkohara@kumamoto-u.ac.jp

References

1. Ferri C, Monti M, La Civita L, et al. Infection of peripheral blood mononuclear cells by hepatitis C virus in mixed cryoglobulinemia. *Blood*. 1993;82:3701-3704.
2. Saito I, Miyamura T, Ohbayashi A, et al. Hepatitis C virus infection is associated with the development of hepatocellular carcinoma. *Proc Natl Acad Sci U S A*. 1990;87:6547-6549.
3. Simonetti RG, Camma C, Fiorello F, et al. Hepatitis C virus infection as a risk factor for hepatocellular carcinoma in patients with cirrhosis. A case-control study. *Ann Intern Med*. 1992;116:97-102.
4. Silvestri F, Pipan C, Barillari G, et al. Prevalence of hepatitis C virus infection in patients with lymphoproliferative disorders. *Blood*. 1996;87:4296-4301.
5. Ascoli V, Lo Coco F, Artini M, Levrero M, Martelli M, Negro F. Extranodal lymphomas associated with hepatitis C virus infection. *Am J Clin Pathol*. 1998;109:600-609.
6. Mele A, Pulsoni A, Bianco E, et al. Hepatitis C virus and B-cell non-Hodgkin lymphomas: an Italian multicenter case-control study. *Blood*. 2003;102:996-999.
7. Dammacco F, Sansonno D, Piccoli C, Racanelli V, D'Amore FP, Lauletta G. The lymphoid system in hepatitis C virus infection: autoimmunity, mixed cryoglobulinemia, and Overt B-cell malignancy. *Semin Liver Dis*. 2000;20:143-157.
8. Inokuchi M, Ito T, Uchikoshi M, et al. Infection of B cells with hepatitis C virus for the development of lymphoproliferative disorders in patients with chronic hepatitis C. *J Med Virol*. 2009;81:619-627.
9. Wakita T, Taya C, Katsume A, et al. Efficient conditional transgene expression in hepatitis C virus cDNA transgenic mice mediated by the Cre/loxP system. *J Biol Chem*. 1998;273:9001-9006.
10. Machida K, Tsukiyama-Kohara K, Seike E, et al. Inhibition of cytochrome c release in Fas-mediated signaling pathway in transgenic mice induced to express hepatitis C viral proteins. *J Biol Chem*. 2001;276:12140-12146.
11. Machida K, Tsukiyama-Kohara K, Sekiguch S, et al. Hepatitis C virus and disrupted interferon signaling promote lymphoproliferation via type II CD95 and interleukins. *Gastroenterology*. 2009;137:285-296, 296 e281-211.

12. Lerat H, Rumin S, Habersetzer F, et al. In vivo tropism of hepatitis C virus genomic sequences in hematopoietic cells: influence of viral load, viral genotype, and cell phenotype. *Blood*. 1998;91:3841-3849.
13. Karavattathayil SJ, Kalkeri G, Liu HJ, et al. Detection of hepatitis C virus RNA sequences in B-cell non-Hodgkin lymphoma. *Am J Clin Pathol*. 2000;113:391-398.
14. Rickert RC, Roes J, Rajewsky K. B lymphocyte-specific, Cre-mediated mutagenesis in mice. *Nucleic Acids Res*. 1997;25:1317-1318.
15. Tanaka T, Lau JY, Mizokami M, et al. Simple fluorescent enzyme immunoassay for detection and quantification of hepatitis C viremia. *J Hepatol*. 1995;23:742-745.
16. Tsukiyama-Kohara K, Tone S, Maruyama I, et al. Activation of the CKI-CDK-Rb-E2F pathway in full genome hepatitis C virus-expressing cells. *J Biol Chem*. 2004;279:14531-14541.
17. Nishimura T, Kohara M, Izumi K, et al. Hepatitis C virus impairs p53 via persistent overexpression of 3beta-hydroxysterol Delta24-reductase. *J Biol Chem*. 2009;284:36442-36452.
18. Tsukiyama-Kohara K, Poulin F, Kohara M, et al. Adipose tissue reduction in mice lacking the translational inhibitor 4E-BP1. *Nat Med*. 2001;7:1128-1132.
19. Fujimura S, Xing Y, Takeya M, et al. Increased expression of germinal center-associated nuclear protein RNA-primase is associated with lymphomagenesis. *Cancer Res*. 2005;65:5925-5934.
20. Miyazaki T, Kato I, Takeshita S, Karasuyama H, Kudo A. Lambda5 is required for rearrangement of the Ig kappa light chain gene in pro-B cell lines. *Int Immunol*. 1999;11:1195-1202.
21. Rubin LA, Galli F, Greene WC, Nelson DL, Jay G. The molecular basis for the generation of the human soluble interleukin 2 receptor. *Cytokine*. 1990;2:330-336.
22. Tsukiyama-Kohara K, Iizuka N, Kohara M, Nomoto A. Internal ribosome entry site within hepatitis C virus RNA. *J Virol*. 1992;66:1476-1483.
23. Jaffe ES, Harris NL, Stein H, Isaacson PG. Classification of lymphoid neoplasms: the microscope as a tool for disease discovery. *Blood*. 2008;112:4384-4399.
24. el-Din HM, Attia MA, Hamza MR, Khaled HM, Thoraya MA, Eisa SA. Hepatitis C Virus and related changes in immunological parameters in non Hodgkin's lymphoma patients. *Egypt J Immunol*. 2004;11:55-64.

25. Feldmann G, Nischalke HD, Nattermann J, et al. Induction of interleukin-6 by hepatitis C virus core protein in hepatitis C-associated mixed cryoglobulinemia and B-cell non-Hodgkin's lymphoma. *Clin Cancer Res.* 2006;12:4491-4498.
26. Mizuochi T, Ito M, Takai K, Yamaguchi K. Differential susceptibility of peripheral blood CD5+ and CD5- B cells to apoptosis in chronic hepatitis C patients. *Biochem Biophys Res Commun.* 2009;389:512-515.
27. Bansal AS, Bruce J, Hogan PG, Prichard P, Powell EE. Serum soluble CD23 but not IL8, IL10, GM-CSF, or IFN-gamma is elevated in patients with hepatitis C infection. *Clin Immunol Immunopathol.* 1997;84:139-144.
28. Rubin LA, Kurman CC, Fritz ME, et al. Soluble interleukin 2 receptors are released from activated human lymphoid cells in vitro. *J Immunol.* 1985;135:3172-3177.
29. Kawamura Y, Ikeda K, Arase Y, et al. Viral elimination reduces incidence of malignant lymphoma in patients with hepatitis C. *Am J Med.* 2007;120:1034-1041.
30. Stamataki Z, Shannon-Lowe C, Shaw J, et al. Hepatitis C virus association with peripheral blood B lymphocytes potentiates viral infection of liver-derived hepatoma cells. *Blood.* 2009;113:585-593.
31. Wasik MA, Sioutos N, Tuttle M, Butmarc JR, Kaplan WD, Kadin ME. Constitutive secretion of soluble interleukin-2 receptor by human T cell lymphoma xenografted into SCID mice. Correlation of tumor volume with concentration of tumor-derived soluble interleukin-2 receptor in body fluids of the host mice. *Am J Pathol.* 1994;144:1089-1097.
32. Tsai MH, Chiou SH, Chow KC. Effect of platelet activating factor and butyrate on the expression of interleukin-2 receptor alpha in nasopharyngeal carcinoma cells. *Int J Oncol.* 2001;19:1049-1055.
33. Yano T, Yoshino I, Yokoyama H, et al. The clinical significance of serum soluble interleukin-2 receptors in lung cancer. *Lung Cancer.* 1996;15:79-84.
34. Tesarova P, Kvasnicka J, Umlaufova A, Homolkova H, Jirsa M, Tesar V. Soluble TNF and IL-2 receptors in patients with breast cancer. *Med Sci Monit.* 2000;6:661-667.
35. Maccio A, Lai P, Santona MC, Pagliara L, Melis GB, Mantovani G. High serum levels of soluble IL-2 receptor, cytokines, and C reactive protein correlate with impairment of T cell response in patients with advanced epithelial ovarian cancer. *Gynecol Oncol.* 1998;69:248-252.

36. Matsumoto T, Furukawa A, Sumiyoshi Y, Akiyama KY, Kanayama HO, Kagawa S. Serum levels of soluble interleukin-2 receptor in renal cell carcinoma. *Urology*. 1998;51:145-149.
37. Pountain G, Hazleman B, Cawston TE. Circulating levels of IL-1beta, IL-6 and soluble IL-2 receptor in polymyalgia rheumatica and giant cell arteritis and rheumatoid arthritis. *Br J Rheumatol*. 1998;37:797-798.
38. Zekri AR, Alam El-Din HM, Bahnassy AA, et al. Serum levels of soluble Fas, soluble tumor necrosis factor-receptor II, interleukin-2 receptor and interleukin-8 as early predictors of hepatocellular carcinoma in Egyptian patients with hepatitis C virus genotype-4. *Comp Hepatol*;9:1.
39. Sheibani K, Winberg CD, van de Velde S, Blayney DW, Rappaport H. Distribution of lymphocytes with interleukin-2 receptors (TAC antigens) in reactive lymphoproliferative processes, Hodgkin's disease, and non-Hodgkin's lymphomas. An immunohistologic study of 300 cases. *Am J Pathol*. 1987;127:27-37.
40. Robb RJ, Rusk CM. High and low affinity receptors for interleukin 2: implications of pronase, phorbol ester, and cell membrane studies upon the basis for differential ligand affinities. *J Immunol*. 1986;137:142-149.
41. Sheu BC, Hsu SM, Ho HN, Lien HC, Huang SC, Lin RH. A novel role of metalloproteinase in cancer-mediated immunosuppression. *Cancer Res*. 2001;61:237-242.
42. Fluckiger AC, Garrone P, Durand I, Galizzi JP, Banchereau J. Interleukin 10 (IL-10) upregulates functional high affinity IL-2 receptors on normal and leukemic B lymphocytes. *J Exp Med*. 1993;178:1473-1481.

Table 1. Lymphoma incidence in HCV-expressing and control mice

HCV expression	Mouse genotype	Number	Incident B-lymphoma, number (%)	Incident T-lymphoma, number (%)
+	RzCD19Cre	72	18 (25.0)	3 (4.1)
-	Rz	34	1(2.9)	1(2.9%)
-	CD19Cre	22	2(9.1)	1(4.5)
-	WT	12	1(8.3)	1(8.3)

Figure Legends

Figure 1. Establishment of RzCD19Cre mice

(A) Schematic diagram of the transgene structure comprised of the complete HCV genome (*HCR6-Rz*). HCV genome expression was regulated by the *Cre/loxP* expression cassette (upper diagram). The Cre transgene was located in the CD19 locus (lower diagram). (B) Expression of HCV core protein in the liver, spleen and plasma of RzCD19Cre mice was quantified by core ELISA. Vertical bars represent the means \pm S.D. (n = 3) (C) Detection of HCV RNA in PBLs by RT-PCR. Samples that included the RT reaction are indicated by “+”, and those that did not include the RT reaction are indicated by “-”. (D) Survival rates of male and female RzCD19Cre mice (male n = 45, female n = 40), Rz mice (male n = 20, female n = 19), CD19Cre mice (male n = 16, female n = 22), and WT mice (male n = 5, female n = 10).

Figure 2. Histopathological analysis of B-cell lymphomas in RzCD19Cre mouse tissues

(A) Histological analysis of tissues from a normal mouse (CD19Cre mouse, ID No. 47-4, male, a, c, e) and a B-cell lymphoma from a RzCD19Cre mouse (ID No. 69-5, male, b, d, f).

Paraformaldehyde-fixed and paraffin-embedded tumor tissues were stained with hematoxylin and eosin (c~f) or immunostained using anti-CD45R (g; lower right, inset) and anti-CD3 (h; lower right, inset). Also shown is a macroscopic view of the lymphoma from a mesenchymal lymph node (b, indicated by forceps), which is not visible in the normal mouse (a). Scale bars: 100 μm (subpanels c, d, g, h) and 20 μm (subpanels e, f, insets in g and h). **(B)** Expression of HCV RNA in B-cell lymphomas from RzCD19Cre mice was examined by RT-PCR. The first round of PCR amplification yielded a 123-bp fragment of HCV cDNA (upper panel), and a second round of PCR amplification yielded a 65-bp fragment (lower panel). The β -actin mRNA was a control. As an additional control, the first and second rounds of amplification were performed using samples that had not been subjected to reverse transcription (RT (-)-HCV). NTC, no template control. **(C)** Ig gene rearrangements in the tumors of RzCD19Cre mice. Genomic DNA isolated from B-cell lymphoma tissues of RzCD19Cre mice (ID Nos. 24-1, 24-4, 54-1, 56-5, 69-5, 31-4, 42-4, 43-4) and spleen tissues of a WT mouse (ID No. 21-2) was PCR-amplified using primers specific for $V\kappa$ - $J\kappa$ genes. Amplification of controls was performed using genomic DNA isolated from a germinal

center-associated nuclear protein (GANP) transgenic mouse (GANP Tg#3) and in the absence of template DNA (NTC). M, DNA ladder marker.

Figure 3. Analysis of serum cytokine and chemokine levels using a multi-suspension array system.

The serum concentration levels of IL-1 α , IL-1 β , IL-2, IL-3, IL-4, IL-5, IL-6, IL-9, IL-10, IL12p40, IL-12p70, IL-13, IL-17, Eotaxin, G-CSF, GM-CSF, IFN- γ , KC, MCP-1, MIP-1 α , MIP-1 β , RANTES, TNF- α , IL-15, FGF-basic, LIF, M-CSF, MIG, MIP-2, PDGF β , and VEGF were measured from the RzCD19Cre mice with B-cell lymphomas (B), T-cell lymphomas (T), and other tumors (mammary tumor, sarcoma, hepatocellular carcinoma) and from tumor-free control RzCD19Cre, Rz, CD19Cre and wild-type (WT) mice.

Figure 4. Serum titers of AST, ALT and soluble IL-2R α in transgenic and control mice lacking or harboring B-cell lymphomas.

(A) The AST assay was performed on serum samples from tumor-free control mice and the RzCD19Cre, Rz, CD19Cre and WT mice with or without B-cell lymphomas or other tumors.

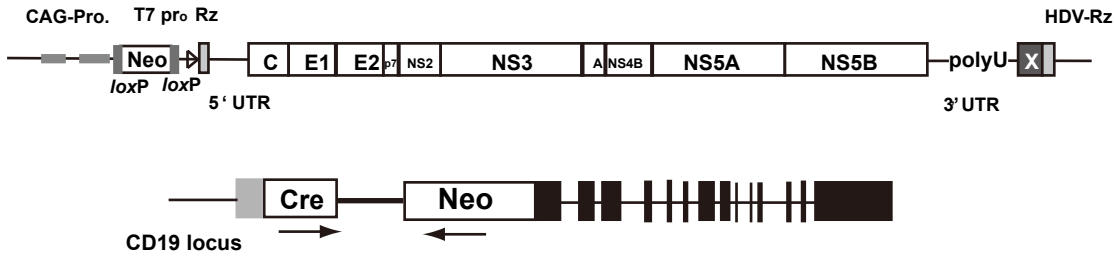
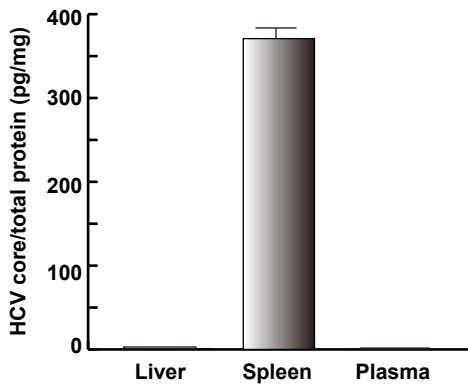
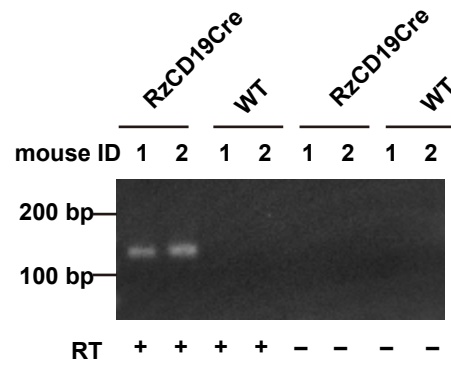
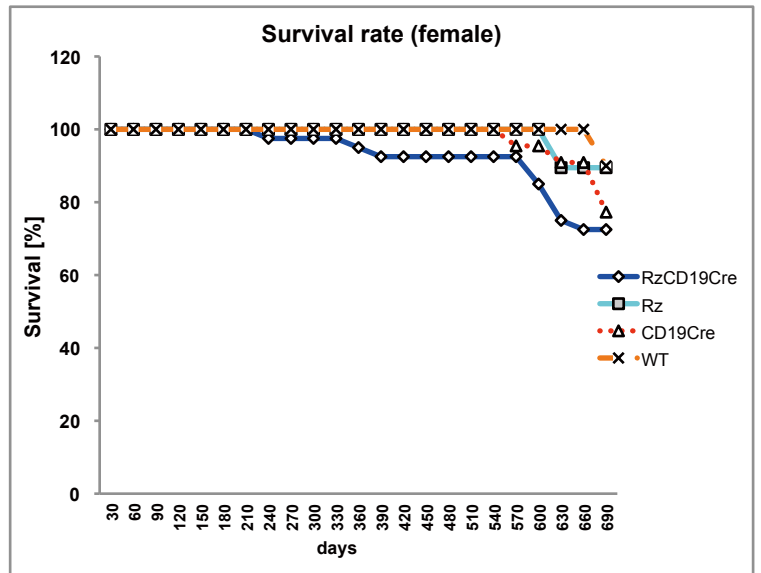
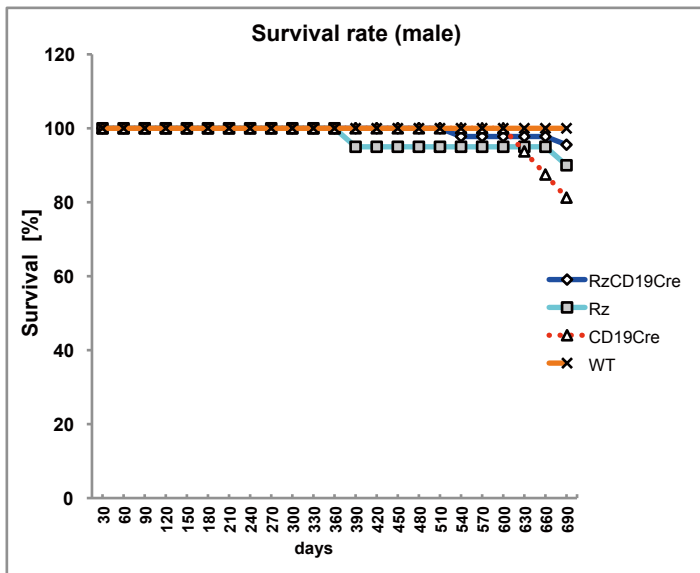
(B) The ALT assay was performed on serum samples from tumor-free control mice and the RzCD19Cre, Rz, CD19Cre and WT mice with or without B-cell lymphomas or other tumors.

(C) ELISA analysis was performed to determine the sIL-2R α concentration in serum samples from tumor-free control mice and the RzCD19Cre, Rz, CD19Cre and WT mice with or without B-cell lymphomas or other tumors.

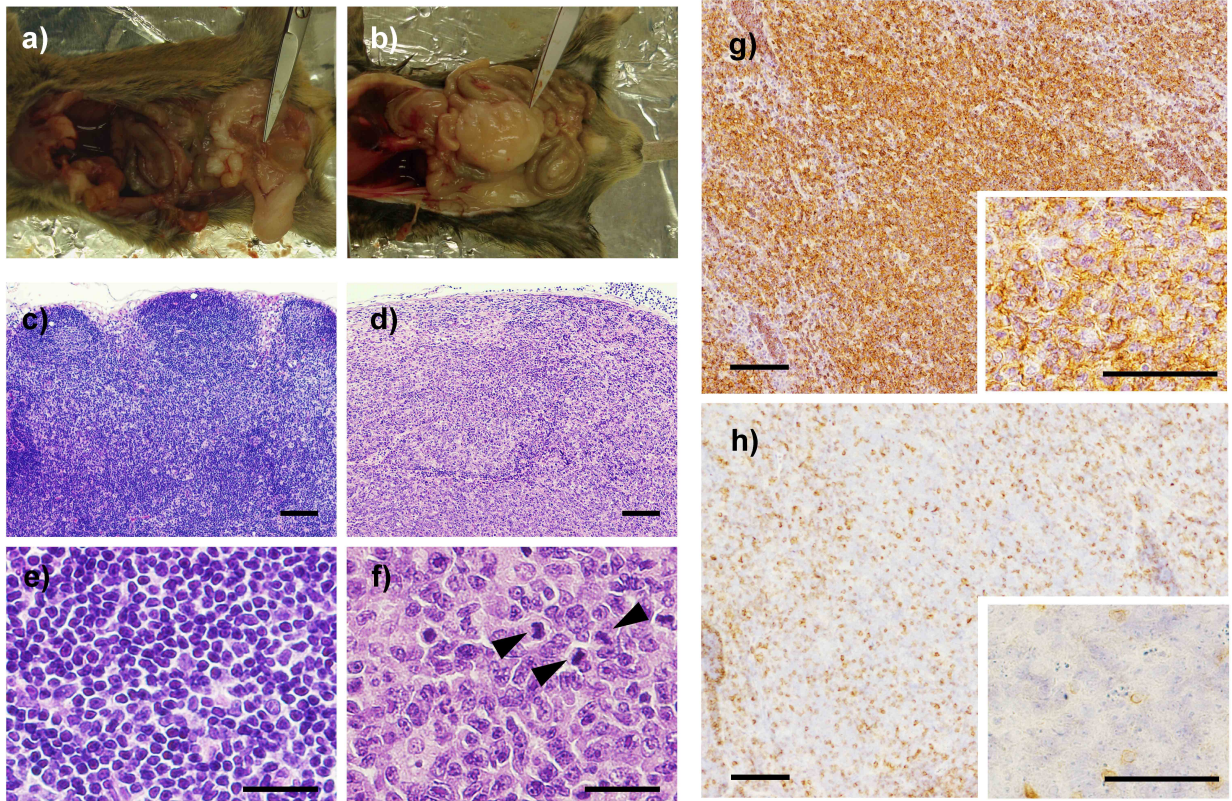
Figure 5. Levels of IL-2R α in transgenic and control mice lacking or harboring B-cell lymphomas.

The expression levels of IL-2R α in splenocytes and PBLs from CD19Cre and RzCD19Cre mice and of B-cell lymphomas from RzCD19Cre mice were measured by ELISA. IL-2R α levels per total protein are indicated (pg/mg). The average of tetrad samples is indicated.

Vertical bars indicate standard deviation. *p < 0.05.

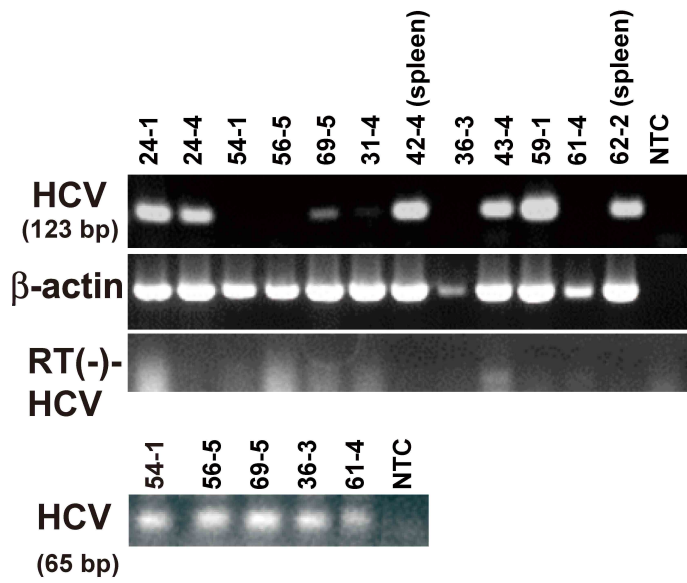
A**HCR6-Rz****B****C****D****Figure.1**

A



B

HCV-RNAs in B-lymphomas



C

V_κ-J_κ

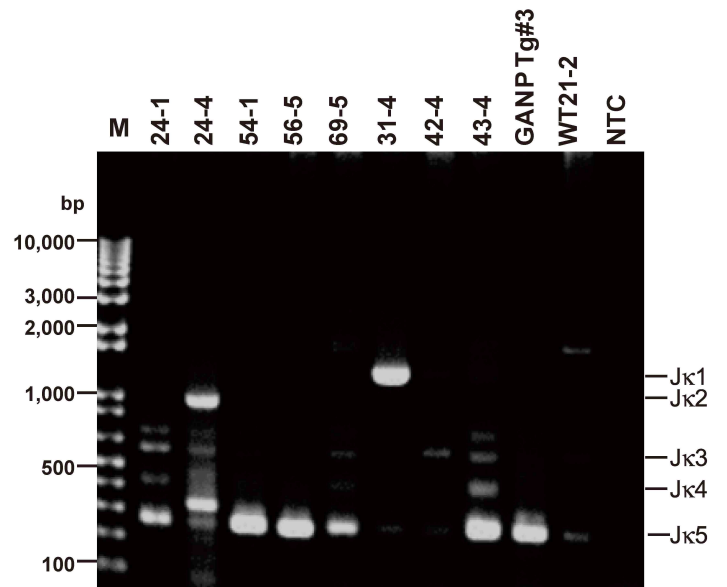


Figure 2

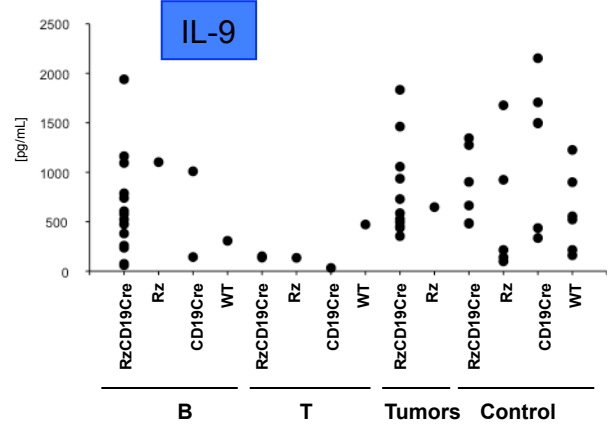
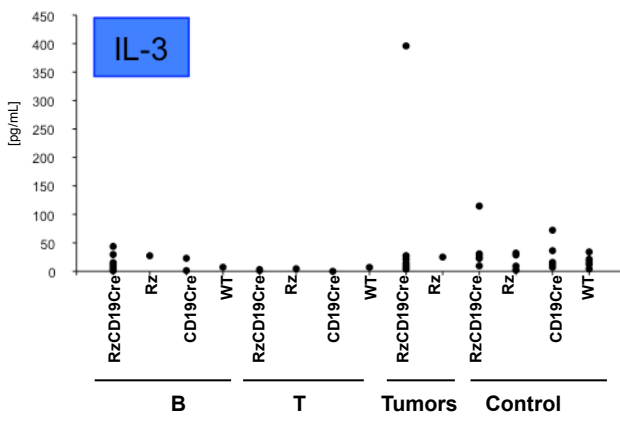
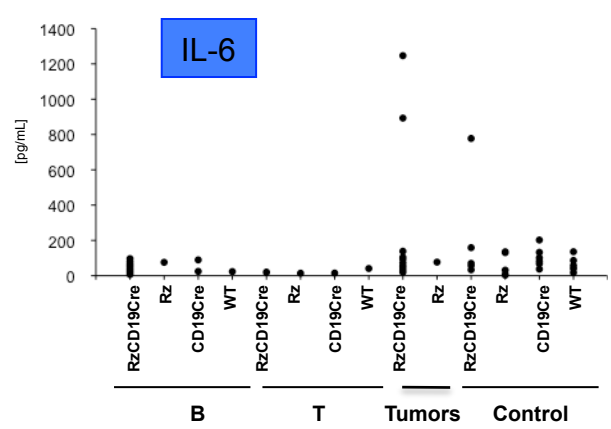
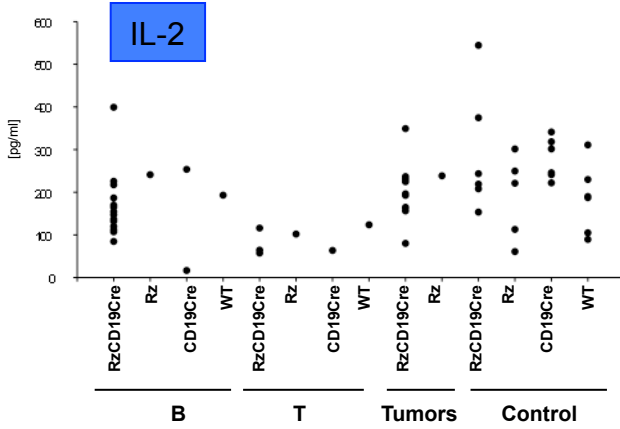
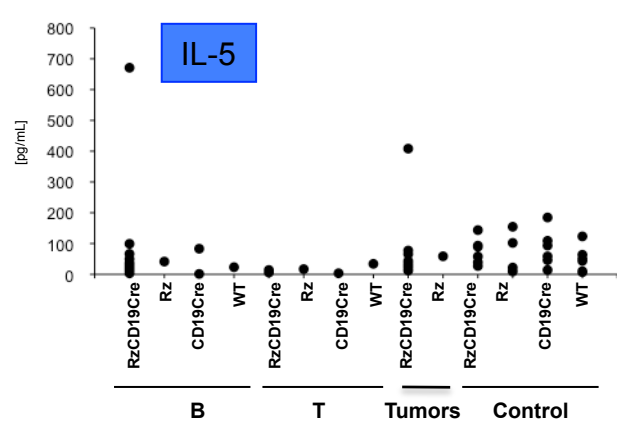
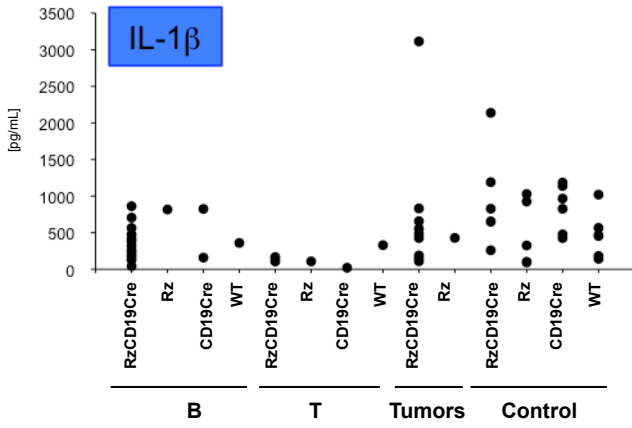
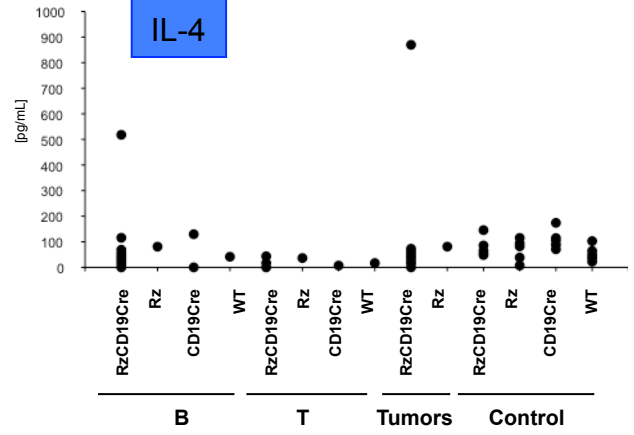
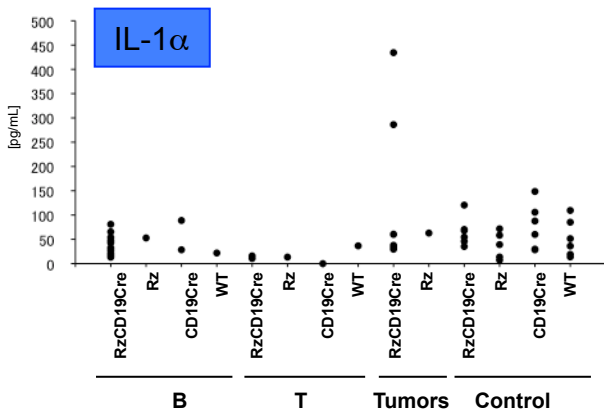


Figure 3

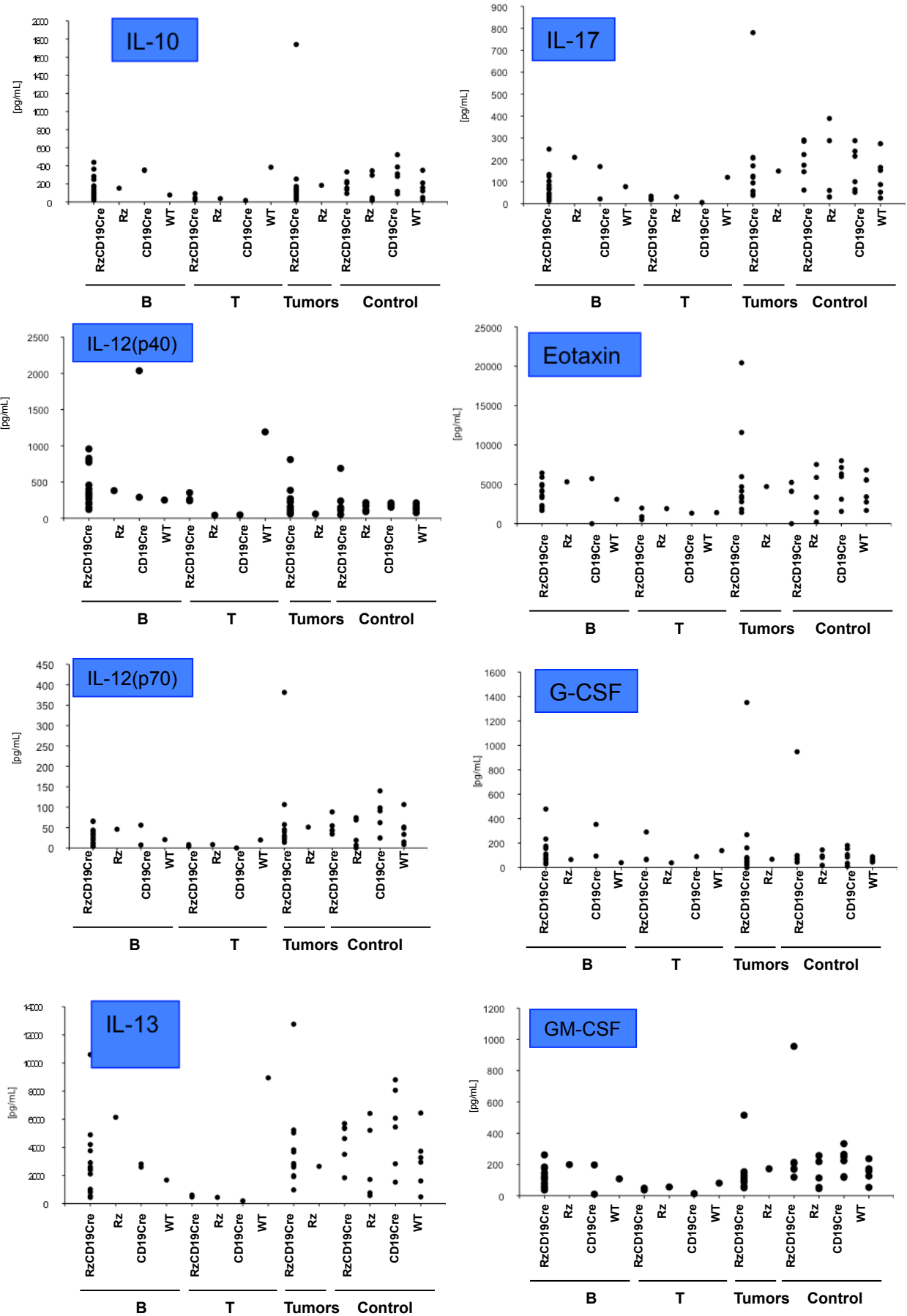


Figure 3

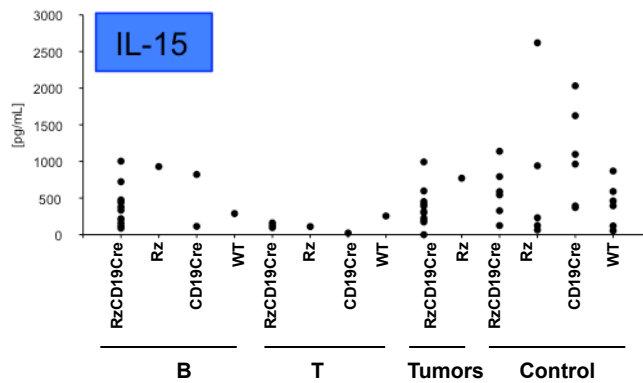
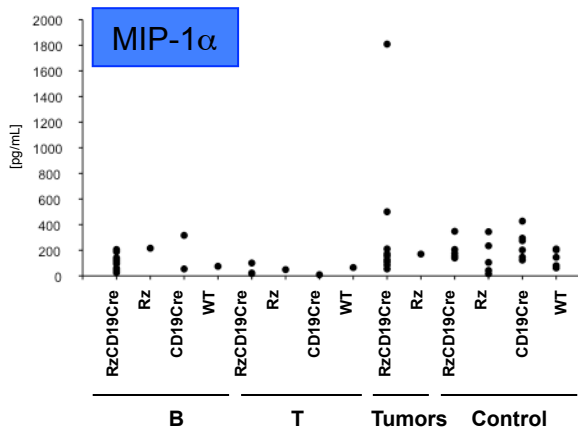
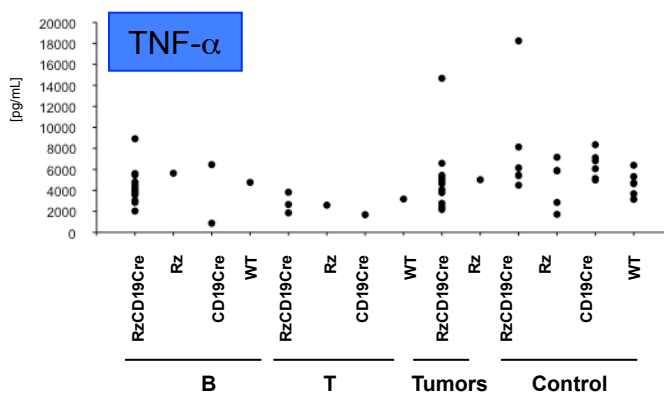
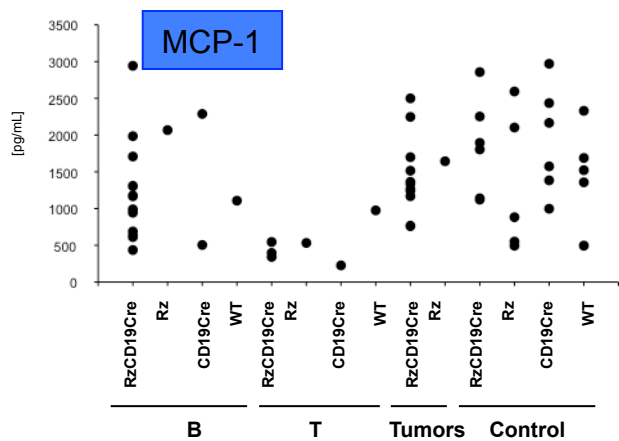
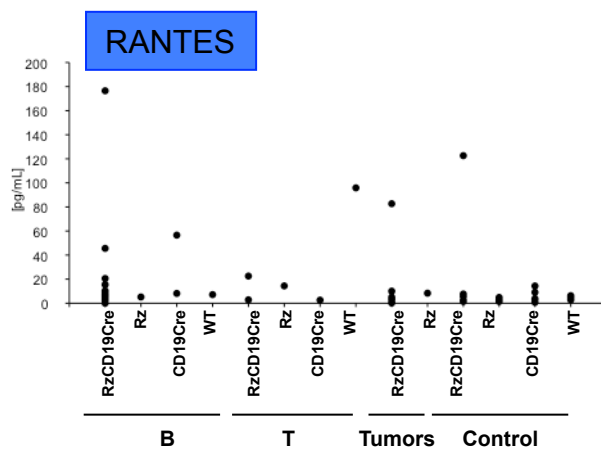
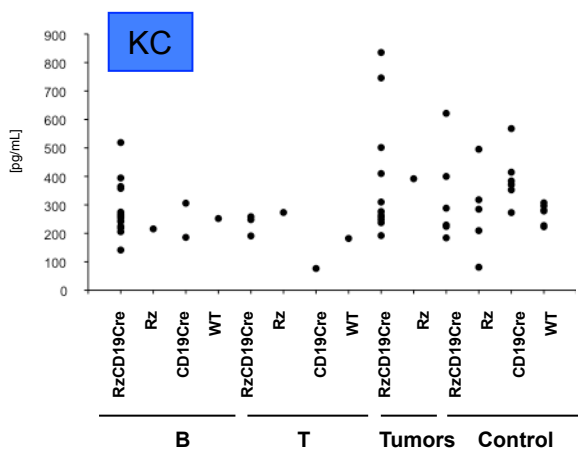
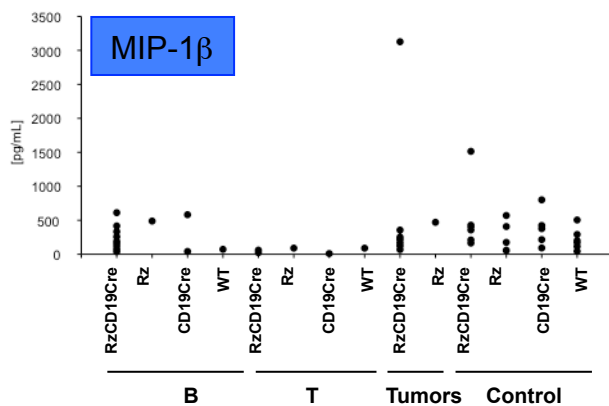
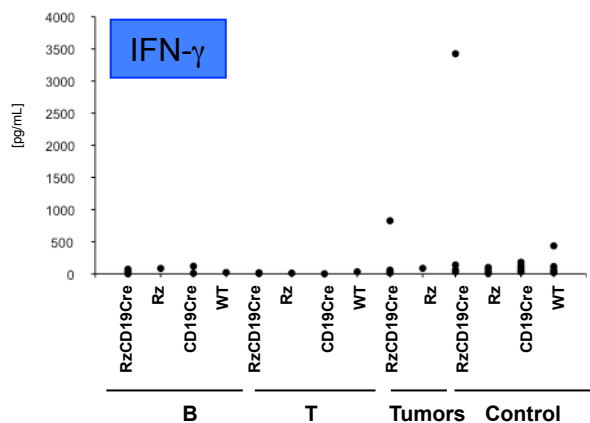


Figure 3

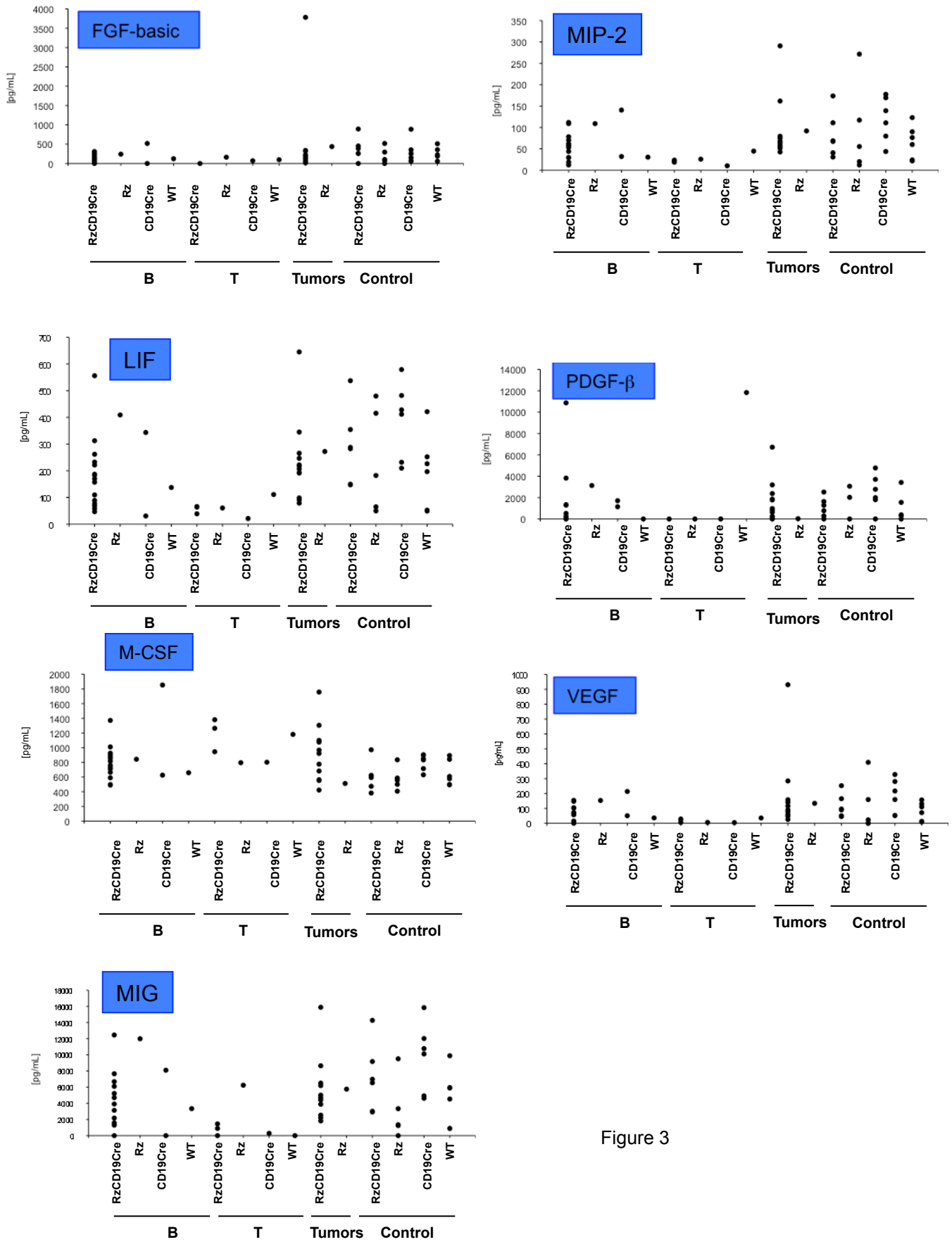
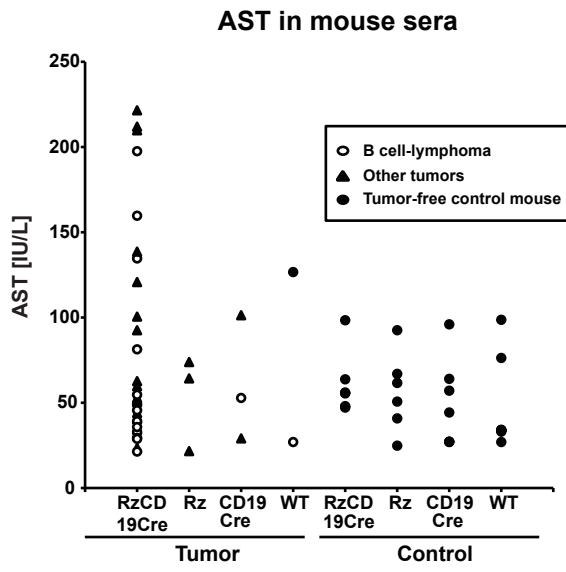
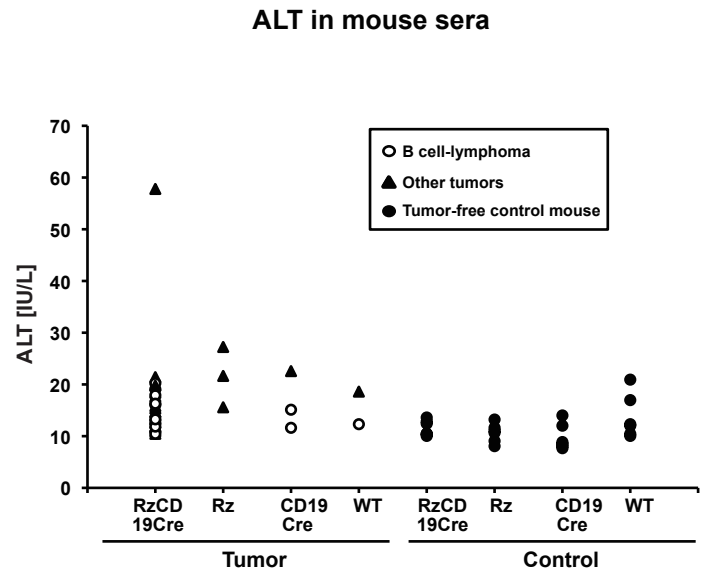
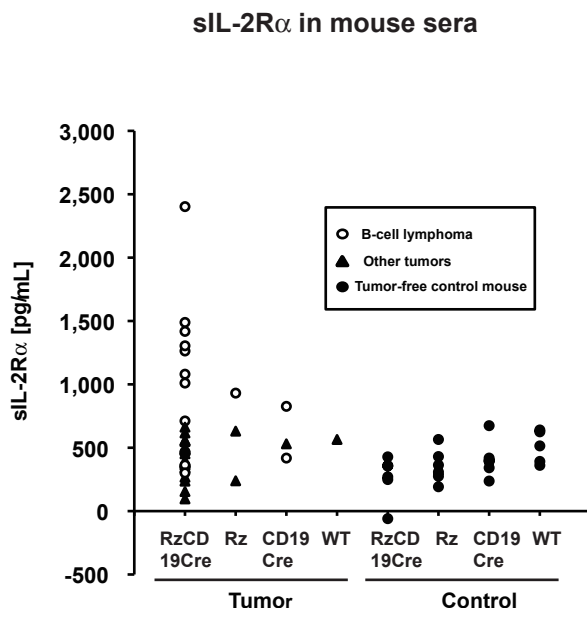


Figure 3

A**B****C****Figure 4**

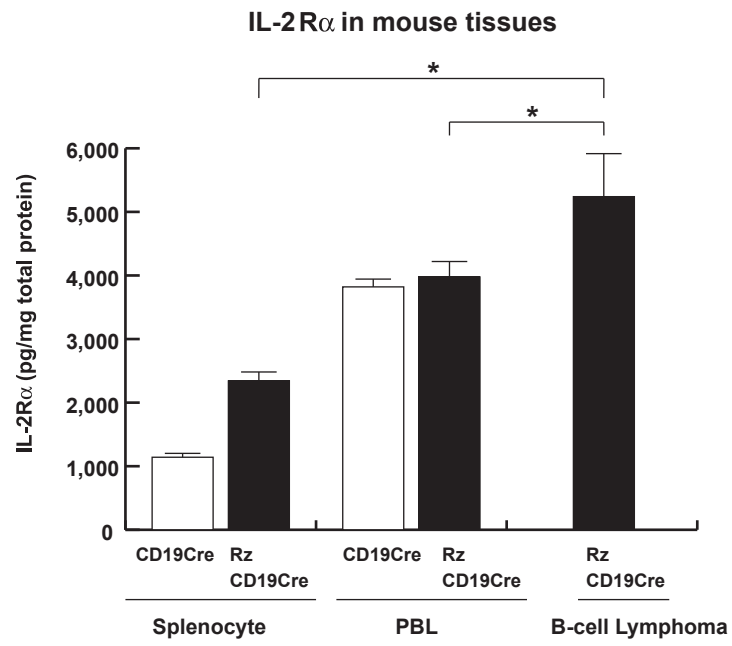


Figure 5